Journal of Power Sources, *24* (1988) 137 - 155

PERFORMANCE TESTING OF 10 kW-CLASS ADVANCED BATTERIES FOR ELECTRIC ENERGY STORAGE SYSTEMS IN JAPAN

M. FUTAMATA*, S. HIGUCHI, O. NAKAMURA, I. OGINO, Y. TAKADA, S. OKAZAKI**, S. ASHIMURA*** and S. TAKAHASHI

Government Industrial Research Institute Osaka, Midorigaoka 1, Ikeda, Osaka, 563 (Japan)

(Received November 18, 1987; in revised form January 15, 1988)

Summary

The results of the performance testing of 10 kW-class advanced batteries — Na–S, Zn–Cl_2, Zn–Br_2 and redox-flow type batteries — are summarized. Energy efficiency and capacity at three discharge rates are presented in addition to energy density, self-discharge rate, estimated short circuit current, etc. It was evident that the performance of the advanced batteries was adequate to achieve the project goals for electrical energy storage. Further improvements are needed in the areas of self-discharge, electric insulation, and auxiliary systems. Based on continued technical progress, there is reasonable expectation that pilot plants of 1 MW (8 MW h) will be constructed and demonstrated in the next phase of the project.

Introduction

Modern a.c. power systems, *e.g.*, oil fired plants, nuclear power plants, have been developed for technical and economical reasons as primary power sources in response to instantaneous electrical load. Electric utilities have two types of a.c. power generating plant — base load plant, and peaking or cycling equipment — to meet fluctuating energy demand in a cost-effective manner. Base load plants are designed to operate for 24 hours each day throughout the year at constant power and to generate low cost electrical power despite the high capital costs. Peaking or cycling equipment is used to meet daily demand peaks. Such equipment is, typically, a low-efficiency,

*Author to whom all correspondence should be addressed.

**Present address: The Graduate School at Nagatsuta, Tokyo Institute of Technology, Midori-ku, Yokohama, 227, Japan.

***Present address: NIIHAMA National College of Technology, Yagumo-cho 7-1, Niihama, 792, Japan.

0378-7753/88/$3.50

fossil-fuel steam plant with gas turbine driven generators. While daily or yearly load variation has been increasing owing to the development of new industries and widely-used air-conditioners, the cost and availability of fossil and distillate fuels are becoming serious problems. In Japan, a typical daily load curve has a 40% midnight factor (ratio of minimum power to peak power), and a typical annual load curve has a 60% load factor (ratio of average power to peak power). These problems could be solved or greatly mitigated if, to cope with fluctuating demand, energy storage systems were used in collaboration with base load plants. If electrical energy was stored at off-peak periods and released at peak periods using energy storage systems, *e.g.*, pumped hydro-electric- and advanced battery systems, etc., the energy output would be controlled according to demand and the load factor would be improved. Consequently, load leveling has become an attractive method from an energy-saving point of view, and the substitution of oil by atomic or other prime-energy sources is expected to become increasingly important. The potential of pumped hydro-electricity appears to be limited due to siting problems, energy density, capital cost, etc. Also, other advanced energy storage systems using compressed air, superconductors, etc., have serious problems yet to be solved. A great deal of attention is therefore being given to advanced secondary batteries as being the most versatile method of storing energy for electric utility systems. The advanced battery shows promise in respect of operative feasibility, flexibility of size and location, rapid response, environmental aspects and economic benefits. These advantages have resulted in active research into, and development of, the advanced battery and energy storage utility.

In Japan, *The Development of an Advanced Battery Electric Power Storage System* was initiated as a national research program within the *Moonlight Project* of 1980 [1, 2]. This project was established by the Agency of Industrial Science and Technology (AIST), the Ministry of International Trade and Industry (MITI), through the national research institutes, and the New Energy Development Organization (NEDO). In this project, high performance advanced batteries and the application of technology to energy storage systems have been studied and developed. Based on this research, a 1 MW (8 MW h) electrical energy storage system will be constructed and tested for the feasibility of its practical application by about 1990 (Fig. 1). The specific performance targets in the 1 MW system are summarized in Table 1. The first phase of the work has been to build and test the 1 kW (8 kW h) modules. The first interim performance test of the 1 kW class batteries — Na–S, $Zn–Cl_2$, $Zn–Br_2$, and the redox-flow type (Cr–Fe) battery — was carried out in 1983 at our Institute. The characteristics of the advanced batteries were discussed and problems to be solved were clarified [3]. The performance was then improved by developing the electrode and electrolyte materials and scaling up the batteries to the 10 kW class; this improvement was undertaken by the five contractors — Yuasa Battery Co., Ltd. and NGK Spark Plug Co., Ltd (Na–S), Furukawa Electric Co., Ltd. ($Zn–Cl_2$), Meidensha Electric Mfg. Co., Ltd. ($Zn–Br_2$), and Mitsui

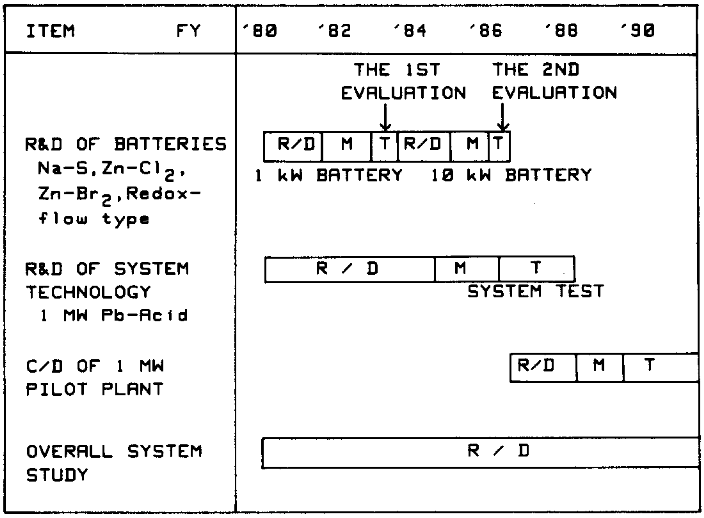

Fig. 1. Research and development schedule of the *Advanced Battery Electric Power Storage System* project. R/D: research, analysis, and design; M: manufacture and construction; T: evaluation test; R&D: research and development.

TABLE 1

Performance goals for the advanced battery system in the project

Item	Performance goals
Capacity	1 MW (8 MW h)
Standard charge/discharge time	8 h/8 h
Overall energy efficiency	More than 70%
Operation life	More than 1500 cycles (More than 10 years)

Eng. & Shipbuilding Co., Ltd. (redox-flow type battery), sponsored by MITI through NEDO.

The performance of the advanced battery must meet the following requirements for the energy storage system:

(i) long cycle life — improvements in corrosion resistance and durability of the electrodes;

(ii) low cost ($/kW h, $/ft^2) — high utilization of active materials, mass production of the battery;

(iii) high a.c./a.c. efficiency — low internal resistance and optimization of the auxiliaries;

(iv) optimization of scale — high current density, and high utilization of the active materials.

Since several of these requirements conflict, approaches have been concentrated on achieving optimized battery systems. Testing and evaluation concepts of the advanced battery not previously considered have been studied at our Institute [4 - 14].

In the next phase of the project, a 1 MW class advanced battery system pilot plant will be constructed from the same type of electrodes and/or unit cells as for the 10 kW class batteries. It was considered that the time was therefore ripe to evaluate the 10 kW class advanced batteries with regard to performance goals, and to review the problems still to be solved. The second interim performance test for 10 kW class advanced batteries was carried out at our Institute between September and December, 1986. The results are detailed in this report.

Experimental

The 10 kW (80 kW h) advanced batteries were tested as detailed below; the battery specifications are summarized in Table 2.

TABLE 2

Specifications for 10 kW class advanced batteries

Battery	Na–S	$Zn–Cl_2$	$Zn–Br_2$	Redox-flow type
Dimensions (m^3)	1.60 × 1.25 × 1.96	1.39 × 1.95 × 2.26	1.37 × 1.59 × 1.67	4.02 × 4.00 × 1.51
Weight (kg)	2465	3138	2915	12820
Unit cell				
Area (cm^2)	495	2800	1600	6000
Current density (mA cm^{-2})	50.5	22.0	13.0	30.8
Voltage (V)	1.8	1.95	1.67	0.9
Capacity (A h/8 HR)	200	495	166	1480
Total numbers	280	96	288	60
Configuration*	(7s × 10p) × 4s	(24s × 2p) × 2p	(24s × 3p) × 4p	30s × 2p
Open circuit voltage (V)	58.0	50.9	43.8	62.0
Charging power (kW)	15.0	14.9	12.7	12.8
Discharging power (kW)				
8 HR	12.5	11.6	10.0	10.0
6 HR	16.0	14.5	13.0	12.8
4 HR	22.5	20.0	19.0	17.4
Contractor	Yuasa Battery Co., Ltd. and NGK Spark Plug Co., Ltd.	Furukawa Electric Co., Ltd.	Meidensha Electric Mfg. Co., Ltd.	Mitsui Eng. & Shipbuilding Co., Ltd.

*s and p denote that the cells are connected in series and parallel, respectively.

(i) Capacity, energy efficiency and energy density

Energy efficiency and capacity were determined at three discharge rates: 8, 6 and 4 h rate (HR) after 8 HR charge. In the second interim evaluation test, the energy efficiency was defined according to Fig. 2 and eqns. (1)

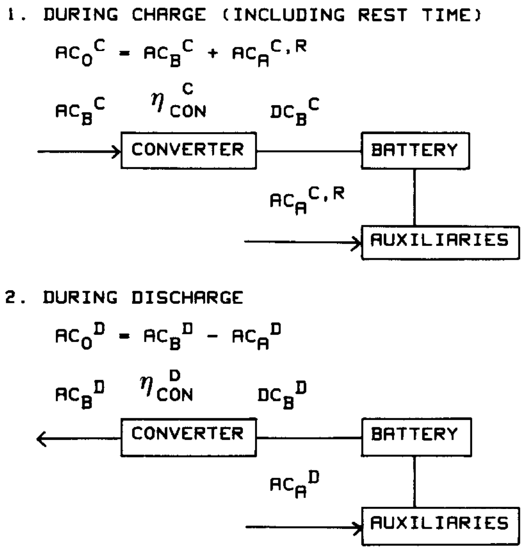

Fig. 2. Energy flow of advanced battery energy storage system. AC_O^C = overall(O) input of a.c. energy; AC_B^C, DC_B^C, AC_A^C = input energy to converter, battery, and auxiliaries, respectively, during charge. Similarly, AC_O^D, AC_B^D, DC_B^D, and AC_A^D refer to the corresponding energy during discharge. $\eta_{CON}^{C,D}$ = efficiency of a.c. - d.c. converter during charge (C) and discharge (D).

and (2). A one-way efficiency of 0.95 for the a.c. - d.c. power converter was used in the following calculations.

(a) Battery efficiency, η_B (d.c./d.c. efficiency), which is calculated from the charged d.c. energy (DC_B^C) and discharged d.c. energy (DC_B^D) of the batteries.

$$\eta_B = \frac{DC_B^D}{DC_B^C} \tag{1}$$

(b) Overall energy efficiency, η_O (a.c./a.c. efficiency), which is determined from the energy consumed by the auxiliaries (AC_A^D, AC_A^C) and the round-trip efficiency of the a.c. - d.c. converter (η_{CON}^C, η_{CON}^D) at charge and discharge, in addition to the stored and extracted energy of the batteries.

$$\eta_O = \frac{AC_O^D}{AC_O^C} = \frac{DC_B^D \eta_{CON}^D - AC_A^D}{\dfrac{DC_B^C}{\eta_{CON}^C} + AC_A^C} \tag{2}$$

$$\left[\begin{array}{l} AC_O{}^D = AC_B{}^D - AC_A{}^D, \quad AC_B{}^D = DC_B{}^D \eta_{CON}{}^D \\ AC_O{}^D\text{: AC output energy from the overall} \\ \quad \text{system during discharge.} \\ AC_O{}^C = AC_B{}^C + AC_A{}^C, \quad AC_B{}^C = DC_B{}^C/\eta_{CON}{}^C \\ AC_O{}^C\text{: AC input energy to the overall} \\ \quad \text{system during charge.} \end{array}\right]$$

In practice, eqn. (2) is valid, because the energy efficiency should be considered as the overall energy storage system. Retained capacity, average current, and energy density were also measured at 8, 6 and 4 HR discharge.

(ii) Cycle life test

Energy efficiency and capacity were observed in relation to charge/discharge cycles at the 8 HR from a reliability point of view.

(iii) Self-discharge rate

To determine the reliability and feasibility of maintenance, the self-discharge rate was found by measuring the capacity after setting aside the fully charged batteries for 24 and 168 h. The electrolytes of the flow type batteries — $Zn-Cl_2$, $Zn-Br_2$ and the redox-flow type battery — were removed from the cell stacks for this test. Because the 8 HR discharge of the batteries could be started within a few minutes, the stand-by state during which the battery was inoperative for a prolonged period, *e.g.*, more than one day, was defined. Thus, the active materials' self-discharge was greatly reduced for these batteries. The decreasing ratios of energy efficiency, $\Delta\eta_O$, $\Delta\eta_B$ were determined by comparing the capacity, after setting aside for 24 and 168 h, with that of a standard 8 HR cycle. The value $\Delta\eta_O$ includes, and $\Delta\eta_B$ excludes, the energy consumed by the auxiliaries. The energy required to keep the batteries in a stand-by state at the operating temperature was also determined; this was called the stand-by energy.

(iv) The starting and stopping time

The time required to start and stop the operation of the batteries was determined to clarify the feasibility of the operation. It was observed from, and to, the waiting period during which the cell stacks were filled with the electrolyte at the operating temperature. The time observed here must be several minutes shorter than that based on the stand-by condition. Self-discharge must be much improved in advance of practical application, therefore the starting and stopping time was observed based on this waiting condition. Also the transition time from the charge mode to discharge at 10 kW was measured.

(v) Transient response properties for load variations

The rise and fall times of the battery system were measured at 8 HR charge and 8, 6, and 4 HR discharge.

(vi) Internal resistance

An a.c. impedance method and a d.c. current step method were adopted to determine the internal resistance of the batteries after removal of the cables from the batteries and the charge/discharge equipment. The initial short circuit battery current was also determined by our method [4, 5].

(vii) Voltage–current characteristics

A *V–I* scan was run on the batteries at 6 states, *i.e.*, the initial, middle, and final stages of the 8 HR charge and discharge. The depths of charge (or discharge) of these stages were 0.5/8, 4/8 and 7.5/8, respectively. The voltage was recorded after 3 min at each current setting. The polarization characteristics of the batteries are discussed.

In addition to the above items, the electrical insulation and the compliance with environmental standards were examined. Table 3 details the accessories of the 10 kW class advanced batteries. Detailed testing conditions are summarized in Table 4. The battery testing facilities were computerized and had a capability for 24-hour-a-day operation. Cycle tests were conducted using the charge/discharge equipment and the microcom-

TABLE 3

The auxiliaries of the 10 kW advanced batteries

	Na–S	Zn–Cl_2	Zn–Br_2	Redox-flow type
Heater	0 - 3[a] (PID[b])			0 - 14 (ON - OFF)
Fan	0 - 0.2 (const.)			
Refrigerator		0.75 (ON - OFF)	0.05 - 0.14 (ON - OFF)	
Pump				
1. Cooling water			0.04 - 0.13 (ON - OFF)	
2. Electrolyte		0.08 - 0.2 (Inverter)	0.25 - 0.75 (const.)	0 - 0.4 (const.)
3. Gas		0.1 (ON - OFF)		
UV lamp		0.04 - 0.08 (ON - OFF)		
Rebalancing				0.12 (ON - OFF)

[a]Numerical values refer to the electric power (kW) consumed by the auxiliaries.
[b]Methods of controlling the auxiliaries' power are shown in parentheses.

TABLE 4

Testing conditions for the 10 kW class advanced batteries

Items		Na–S	$Zn-Cl_2$	$Zn-Br_2$	Redox-flow type
1. Energy efficiency					
Charge					
Power (kW)		15.0	14.9	12.7	12.8
Duration (h)		8	8	8	8
Discharge					
Power (kW)	8 HR	12.5	11.6	10.0	10.0
(c.o.v.*, V)		(12.5)	(24.0)	(24.0)	(48.0)
	6 HR	16.0	14.5	13.0	12.8
		(16.0)	(24.0)	(24.0)	(45.0)
	4 HR	22.5	20.0	19.0	17.4
		(22.5)	(24.0)	(24.0)	(43.0)
2. Rate of self-discharge; standing time (h): 24 and 168					
3. Life cycle; energy efficiency in relation to 8 HR cycles					
4. Internal resistance					
a.c. impedance method: input voltage = 10 mV, 0.01 Hz–20 kHz					
d.c. current step method: input voltage = 5 - 100 mV					
5. *V–I* characteristics; voltage after 3 min duration of rated current					
during charge (A)		0 - 300	0 - 500	0 - 500	0 - 400
during discharge (A)		0 - 600	0 - 600	0 - 500	0 - 600
6. Starting and stopping time; time for starting 8 HR operation from cooled down and stand-by state, and for stopping to stand-by state					
7. Electrical insulation; d.c. 3000 V (1 min) between an electrode and container					

*Cut-off voltage.

puter. The computer automatically monitored battery voltage, current, and temperature, and served as a controller and data acquisition device. Ampere hours and watt hours were integrated over the sampling interval. Other testing equipment was designed and constructed in advance of the second interim performance test.

Results and discussion

The evaluation testing results are summarized in this section. Detailed results will be published elsewhere [15 - 17].

(i) Capacity, energy efficiency and energy density

Figures 3 and 4 show the charge and discharge curves at 8, 6, and 4 HR. The discharge capacity of the batteries exceeded the target of 8 h at

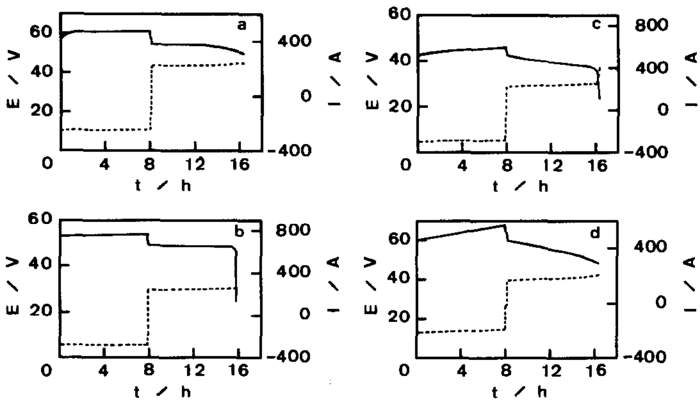

Fig. 3. Charge and discharge curves at 8 HR discharge. ——, Voltage; - - - -, current. Curves a, b, c, and d refer to Na–S, $Zn–Cl_2$, $Zn–Br_2$, and redox-flow type battery, respectively.

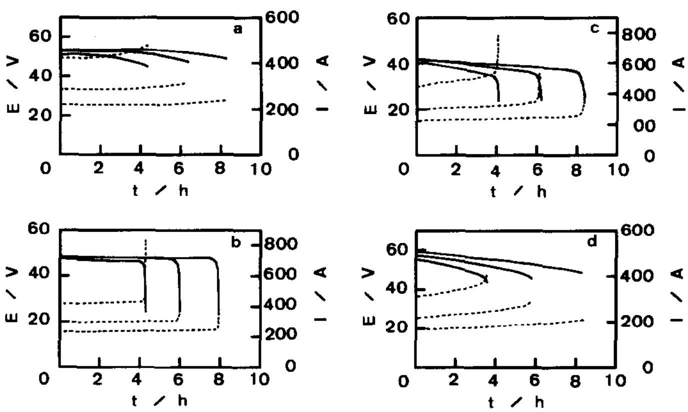

Fig. 4. Discharge curves at the rated discharge. Symbols are as in Fig. 3.

the nominal power. The battery efficiency (η_B) and overall efficiency (η_O) are summarized for three discharge rates in Tables 5 and 6. The overall efficiency at 8 HR was observed as 77.1, 65.7, 71.1, and 69.4% for Na–S, $Zn–Cl_2$, $Zn–Br_2$, and the redox-flow type battery, respectively. As shown in Table 7, the 10 kW battery efficiency was much improved in comparison with those of the 1 kW class batteries in spite of the scale-up [3]. The battery efficiency and overall efficiency are expected to attain the goal of 80 and 70%, respectively.

The overall efficiency was determined for one cycle, η_O, excluding the energy consumed by the auxiliaries during rest time after discharge. The rest time clearly depends on the operation cycle. For practical purposes, the energy efficiency should be given as a daily, $\eta_{O,D}$, and weekly operation, $\eta_{O,W}$. The efficiencies of $\eta_{O,D}$ and $\eta_{O,W}$ were estimated for the appropriate

TABLE 5

Energy efficiency and capacity of 10 kW class Na–S and $Zn–Cl_2$ batteries at three discharge rates

Mode	Na–S			$Zn–Cl_2$		
Discharge rate (HR)	8	6	4	8	6	4
Charge						
duration (h)	7.998	7.993	7.990	8.000	8.000	8.000
energy (kW h)						
battery	119.902	119.831	119.793	119.197	119.185	119.178
aux.*	2.973	1.195	0.930	4.893	5.708	5.157
Rest after charge						
energy (kW h) aux.*	0.013	0.026	0.011	0.041	0.011	0.028
Discharge						
duration (h)	8.442	6.466	4.399	8.018	6.059	4.324
energy (kW h)						
battery	105.516	103.476	99.031	92.964	87.813	86.452
aux.*	0.590	0.499	0.561	1.573	2.728	1.234
Rest after discharge						
energy (kW h) aux.*	0.000	0.000	0.000	1.595	2.278	2.896
Efficiency						
η_B (%)	88.00	86.35	82.67	77.99	73.68	72.54
η_O (%)	77.13	76.79	73.61	65.71	60.47	60.58
Energy density						
(kW h m^{-2})	52.46	51.49	49.24	33.72	31.39	31.44
(kW h m^{-3})	26.77	26.27	25.12	14.92	13.89	13.91
(W h kg^{-1})	42.57	41.78	39.95	29.12	27.11	27.16

*Auxiliaries.

operation schedules, as shown in Table 8. Small differences were observed between the three kinds of energy efficiencies for the $Zn–Cl_2$ and $Zn–Br_2$ batteries because of the small amount of stand-by energy. However, for Na–S and the redox-flow type battery, the daily and weekly efficiencies were remarkably less than the efficiency of a single cycle, η_O, because of the large stand-by energy. The energy per footprint area, volume, and weight, was calculated for the capacity at the 8 HR discharge as shown in Tables 5 and 6. The Na–S battery showed the highest values of all the energy densities in the four types of battery. By contrast, all the forms of energy density of the redox-flow type battery were smaller by an order of magnitude than those of the other three batteries because of the large quantity of redox solution — 8 m^3. The capacity of the redox-flow type battery decreased as the discharge rate increased. This is possibly because the electrolyte circulating pump was underpowered.

TABLE 6

Energy efficiency and capacity of 10 kW class $Zn-Br_2$ and redox-flow type batteries at various discharges

Mode	$Zn-Br_2$			Redox-flow type		
Discharge rate (HR)	8	6	4	8	6	4
Charge						
duration (h)	8.002	8.002	8.002	8.002	8.002	8.002
energy (kW h)						
battery	101.555	101.457	101.498	102.099	102.082	102.087
aux.*	1.910	1.903	1.907	2.714	2.663	2.918
Rest after charge						
energy (kW h) aux.*	0.015	0.011	0.011	0.047	0.028	0.033
Discharge						
duration (h)	8.373	6.147	4.093	8.348	5.739	3.564
energy (kW)						
battery	83.645	79.854	77.739	83.475	73.458	62.022
aux.	2.011	1.559	1.510	2.811	1.912	1.211
Rest after discharge						
energy (kW h) aux.*	0.087	0.058	0.087	0.000	0.000	0.000
Efficiency						
η_B (%)	82.36	78.71	76.59	81.76	71.96	60.75
η_O (%)	71.11	68.31	66.46	69.39	61.62	52.27
Energy density						
(kW h m^{-2})	37.48	35.95	35.00	5.016	4.449	3.782
(kW h m^{-3})	22.45	21.52	20.95	3.322	2.947	2.504
(W h kg^{-1})	28.00	26.86	26.15	6.292	5.581	4.743

*Auxiliaries.

TABLE 7

Comparison of battery efficiency in the first ($\eta_{B,1st}$) and second ($\eta_{B,2nd}$) interim evaluation tests

	Na–S	$Zn-Cl_2$	$Zn-Br_2$	Redox-flow type
$\eta_{B,1st}$ (%)	85.9	71.1	80.1	76.7
$\eta_{B,2nd}$ (%)	88.0	78.0	82.4	81.8

(ii) Cycle life characteristics

Cycle life tests were continued to attain the goal of 1500 cycles. The battery, η_B, and overall η_O, energy efficiencies for 10 kW class advanced batteries are shown in relation to cycle number from October 1986 to September 1987 in Table 9 and Figs. 5 and 6. The battery and the overall efficiencies were almost maintained at the initial level, and little performance deterioration was observed for the four types of advanced batteries. The

TABLE 8

Overall energy efficiency for the single cycle η_O, daily cycle $\eta_{O,D}$ and weekly cycle $\eta_{O,W}$ of 10 kW class advanced batteries

	Na–S	Zn–Cl_2	Zn–Br_2	Redox-flow type
η_O (%)	77.1	65.7	71.1	69.4
$\eta_{O,D}$* (%)	75.7	65.1	70.7	67.7
$\eta_{O,W}$** (%)	71.4	64.3	70.7	63.2

*Calculated for the schedule: 1 day = charge (8 h) + rest (2 h) + discharge (8 h) + rest (6 h).
**Calculated for the schedule: 1 week = 5 days' operation + 2 days' rest.

TABLE 9

The battery efficiency (η_B) and overall efficiency (η_O) of 10 kW class advanced batteries in the second cycle life test (as at the end of September 1987)

	Na–S	Zn–Cl_2	Zn–Br_2	Redox-flow type
Initial efficiency				
η_B (%)	85.7	78.1	79.7	78.6
η_O (%)	77.0	66.2	68.4	66.1
Current status*				
No. of cycles	380	268	257	257
η_B (%)	83.0	76.6	78.5	78.1
η_O (%)	74.8	64.6	67.2	66.1

* In progress.

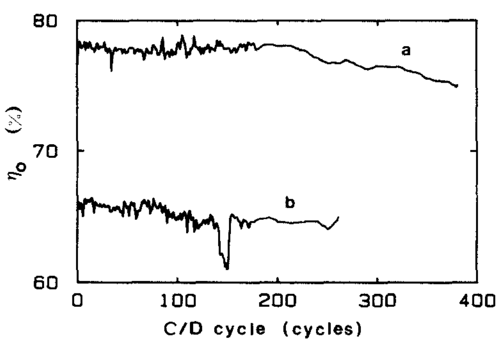

Fig. 5. C/D cycle dependence of overall energy efficiency, η_O, from October 1986 to September 1987. Symbols are as in Fig. 3. After 170th cycle, average values for each 10 cycles are plotted.

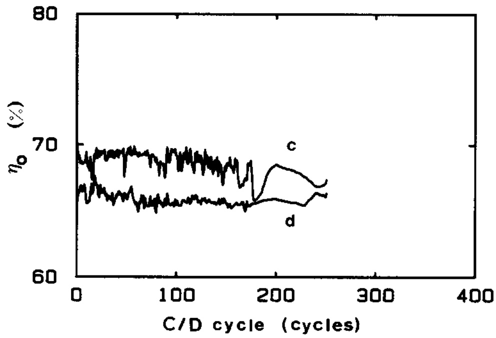

Fig. 6. C/D cycle dependence of overall energy efficiency, η_O, from October 1986 to September 1987. Symbols are as in Fig. 3. After 170th cycle, average values for each 10 cycles are plotted.

TABLE 10

The battery efficiency (η_B) of 1 kW class advanced batteries in the first cycle life test (as at the end of September 1987)

	Na–S	Zn–Cl_2	Zn–Br_2	Redox-flow type
Initial efficiency, η_B (%)	85.9	71.1	80.1	76.7
Current status*				
No. of cycles	1059	655	597	859
η_B (%)	68.4	72.4	75.0	65.8

*In progress.

results of the first interim life cycle test are given in Table 10. All the 1 kW class version batteries have attained 500 cycles and retained a battery efficiency of some 70%.

(iii) Self-discharge rate

The goals for $\Delta\eta_O$ and $\Delta\eta_B$ were set at 5% of the 8 HR capacity after standing for one week. By removing the electrolyte from the cell stacks for the flow type batteries, the rate was dependent on the stand-by energy and/or the remaining electrolyte in the cell stacks. The decreasing ratios of capacity and battery efficiency, η_B, for the four batteries were rather low, as shown in Tables 11 and 12, by comparison with ordinary Pb–acid batteries. The stand-by energy was larger for the Na–S (19.4 kW h/day) and the redox-flow type battery (20.1 kW h/day) than for the Zn–Cl_2 (0.7 kW h/day) and the Zn–Br_2 battery (0.0 kW h/day). Therefore, the decreasing ratio of the overall efficiency, $\Delta\eta_O$, including energy consumed by the auxiliaries, was very large for these batteries. The Na–S and the redox-flow type batteries are suitable for daily operation for load leveling purposes.

TABLE 11

Rate of self-discharge of 10 kW class Na–S and $Zn-Cl_2$ batteries

	Na–S		$Zn-Cl_2$	
Standing time (h)	24	168	24	168
Charge energy (kW h)				
battery	119.918	119.929	119.183	119.167
aux.*	4.703	4.654	4.551	4.955
Rest after charge energy (kW h) aux.*	17.999	136.096	0.117	4.738
Discharge energy (kW h)				
battery	105.402	105.410	89.832	88.941
aux.*	0.601	0.589	1.694	1.681
Rest after discharge energy (kW h) aux.*	0.000	0.000	1.9122	2.362
Battery efficiency η_B (%)	87.90	87.89	75.37	74.64
Overall efficiency η_O (%)	66.83	37.29	63.35	60.23
Decreasing rate of capacity (% h^{-1})	0.00	0.00	0.15	0.03
Decreasing ratio of η_B (%)	0.11	0.12	3.36	4.30
Decreasing ratio of η_O (%)	13.35	51.66	3.59	8.34
Stand-by energy (kW h h^{-1})	0.750	0.810	0.0049	0.0282

*Auxiliaries.

However, these batteries should not be used for urgent power sources which must be retained at the operating temperature thereby consuming the stand-by energy. By contrast, $Zn-Cl_2$ and $Zn-Br_2$ batteries are applicable, even in this instance.

(iv) Starting and stopping time

The times necessary to start and stop the operation, and also to switch from charge to discharge, were measured. The starting and stopping times at the operating temperature were observed to be within 1 s for Na–S, $Zn-Br_2$ and the redox-flow type battery and about 2 min for the $Zn-Cl_2$ battery. It was confirmed that the advanced battery system is started and stopped in a much shorter time than that of a hydroelectric power plant (several min). Since Na–S and redox-flow type batteries are operated at 350 °C and 35 - 40 °C, respectively, a warming-up period from the cooled state is necessary. The time was noted as 87.5 and 24.9 h for the Na–S and the redox-flow type battery, respectively. The switching from charge to discharge was quickly accomplished for all the batteries except $Zn-Cl_2$, whose reservoir of solvated chlorine must be cooled just before charge.

TABLE 12

Rate of self-discharge of 10 kW class Zn–Br_2 and redox-flow type batteries

	Zn–Br_2		Redox-flow type	
Standing time (h)	24	168	24	168
Charge energy (kW h)				
battery	101.574	101.545	102.072	102.058
aux.*	1.943	1.900	2.717	2.893
Rest after charge energy (kW h) aux.*	0.080	0.043	20.764	140.764
Discharge energy (kW h)				
battery	77.945	77.428	78.691	78.973
aux.*	1.852	1.819	2.664	2.680
Rest after discharge energy (kW h) aux.*	0.051	0.051	0.000	0.000
Efficiency				
η_B (%)	76.74	76.25	77.09	77.38
η_O (%)	66.24	65.88	55.06	28.81
Decreasing rate of capacity (% h^{-1})	0.283	0.044	0.239	0.0321
Decreasing ratio of η_B (%)	6.82	7.42	5.71	4.83
Decreasing ratio of η_O (%)	6.85	7.35	20.65	58.48
Stand-by energy (kW h h^{-1})	0.0034	0.00025	0.865	0.838

*Auxiliaries.

The time for the Zn–Cl_2 battery should be reduced by automating the bulb switching for controlling the Cl_2 gas pressure and optimising the refrigeration. The stopping time was observed to be within 1 s for all the advanced batteries.

(v) Transient response properties for load variation [15]

The rise and fall times of the battery systems (battery and C/D cycler) were observed as being within 20 and 1 ms, respectively, as shown in Fig. 7 and Table 13. The response time is determined by the impedance characteristics of the overall systems. It was independent of battery type and state of charge, because the impedances of the overall battery systems were not affected by the batteries, but by the cycler and cable, etc. The results indicate that the battery systems respond quickly to irregular and large load fluctuations.

(vi) Internal resistance

The resistance was measured and the initial short circuit current estimated, as shown in Table 14. The impedance characteristics of the 10 kW class module batteries were much different from those of unit cells [16],

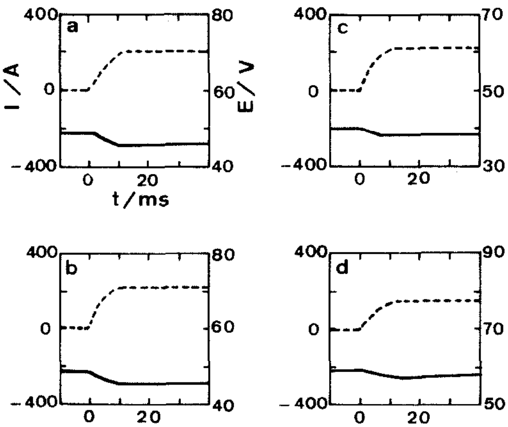

Fig. 7. Transient characteristics (rising) of the 10 kW class advanced batteries at 8 HR charge. Symbols are as in Fig. 3.

TABLE 13

Apparent response time of the 10 kW class batteries

Measurement point		Response time[a] (ms)				
		Na–S	$Zn–Cl_2$	$Zn–Br_2$	Redox-flow	Pb–acid
8 HR charge	rise[b]	14	8	19	13	18
	fall[c]	0.4	0.4	0.4	0.4	0.2
8 HR discharge	rise	10	7	7	9	11
	fall	1	1	2	1	0.5
6 HR discharge	rise	10	6	7	10	
	fall	0.7	2	3	0.5	
4 HR discharge	rise	10	6	8	8	
	fall	0.8	2	2	0.8	

[a]Time for the current to change from 10 to 90% of rated values and containing that of the C/D equipment.
[b,c]Rise and fall times were measured, respectively, at the start and finish of rated charge or discharge.

and scarcely depended on states of charge. This is probably because the capacitance of the plate electrodes parallel to each other and the inductance of the terminal and manifold between the unit cells are dominant in the internal resistance of the batteries.

(vii) Voltage–current characteristics [17]

The results showed that the polarization characteristics of the batteries were essentially linear over a wide current range for both charge and dis-

TABLE 14

Internal resistance and short circuit current of 10 kW class advanced batteries

	Na–S	Zn–Cl_2	Zn–Br_2	Redox-flow type
Internal resistance				
a.c. method (mΩ)	14	12	12	17
d.c. method (mΩ)	13	11	12	16
Initial short circuit current				
a.c. method (A)	4100	4200	3500	3500
d.c. method (A)	4400	4600	3500	3700

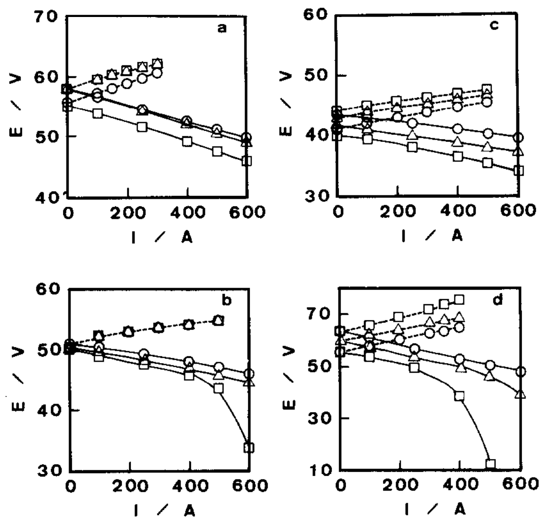

Fig. 8. Voltage–current curves of the 10 kW class advanced batteries. Curves a, b, c, and d are as in Fig. 3. Symbols ○, △, and □ refer to the initial (0.5/8), middle (4/8) and final (7.5/8) stages of the 8 HR charge and discharge, respectively. (The depth of charge or discharge of the stages are shown in parentheses.) - - - -, charge; ——, discharge.

charge, indicating a predominantly ohmic impedance of about 10 mΩ (Fig. 8). The values were consistent with those observed in Section (vi). It was also verified that the advanced batteries were amenable to high rate discharges up to 600 A and charges of 300 - 500 A.

The electrical insulation between an electrode and cell container was tested after removing the cables of auxiliaries and sensors, because these elements were not optimized at this stage. The results showed that improvements in insulation are still necessary for the overall battery systems. Concentrations of poisonous gases, such as SO_2 (Na–S), Cl_2 (Zn–Cl_2), Br_2 (Zn–Br_2) and HCl (redox-flow type), were monitored both inside and outside the testing rooms over the testing period. No gas contents above the environmental standards of Japan were detected. No safety problems were

TABLE 15

Characteristics and problems of the 10 kW class advanced batteries

Battery	Advantage	Problem
Na–S	1. Very high energy efficiency (η_O = 77.1%) 2. No self-discharge 3. Remarkably high energy density (52.5 kW m^{-2}, 26.8 kW h m^{-3}, 42.6 W h kg^{-1})	1. Large stand-by energy (19.4 kW h day^{-1}) 2. Temperature control system necessary 3. Reliability and high cost of solid electrolyte
$Zn–Cl_2$	1. Stable voltage during charge and discharge 2. Little stand-by energy (0.7 kW h day^{-1})	1. Rather low energy efficiency (65.7%) 2. Complex solvation technique for efficient operation 3. High auxiliaries' power 4. Low energy density 5. Dendritic zinc deposition
$Zn–Br_2$	1. High energy efficiency (η_O = 71.1%) 2. Little stand-by energy (0.0 kW h day^{-1}) 3. Temperature control is unnecessary 4. Low cost electrode	1. High self-discharge rate ($\Delta\eta_B$ = 7.4% $week^{-1}$) 2. Dendritic zinc deposition
Redox-flow type	1. Long operational life is expected because active materials neither deposit nor dissolve	1. Low energy density (5 kW h m^{-2}, 3.3 kW h m^{-3}, 6.3 W h kg^{-1}) 2. Large stand-by energy (20.1 kW h day^{-1}) 3. Temperature control system necessary (40 °C)

encountered with these batteries, but halogen gas scrubbing systems were occasionally needed to cope with minor halogen gas releases from the $Zn–Cl_2$ and $Zn–Br_2$ batteries. Finally, the current status, and the problems to be overcome in respect of the 10 kW class advanced batteries are summarized in Table 15. The reliability, safety, and economic assessments of the total battery systems should be established in advance of practical applications; these are outside the scope of this investigation.

Conclusion

It is evident that the performance of the four 10 kW class advanced batteries developed in Japan is sufficient to achieve the project goals —

energy efficiency, cycle life, *I–V* characteristics, fast response, etc. However, improvements are needed in the areas of self-discharge, electrical insulation, and auxiliary systems via engineering and manufacturing process developments in the future. Based on continued technical progress, it is reasonable to expect that pilot plants of 1 MW/8 MW h will be constructed and demonstrated in the final phase of this project.

References

1 S. Takahashi and T. Hiramatsu, *J. Power Sources, 17* (1986) 55.
2 New Energy Development Organisation, *Annu. Rep. for FY 1984*, 1985.
3 S. Higuchi, S. Okazaki, I. Ogino, O. Nakamura, Y. Takada and S. Takahashi, *Bull. Gov. Indust. Res. Inst., Osaka, 36* (1985) 100.
4 S. Okazaki, S. Higuchi, N. Kubota and S. Takahashi, *J. Appl. Electrochem., 16* (1986) 513.
5 S. Okazaki, S. Higuchi, N. Kubota and S. Takahashi, *J. Appl. Electrochem., 16* (1986) 631.
6 S. Okazaki, S. Higuchi, O. Nakamura and S. Takahashi, *J. Appl. Electrochem., 16* (1986) 894.
7 M. Futamata and S. Takahashi, *J. Phys. E; Sci. Instrum., 20* (1987) 1351.
8 S. Takahashi and S. Okazaki, *Prog. Batt. Sol. Cells, 5* (1984) 161.
9 S. Higuchi, S. Takahashi and S. Okazaki, *Prog. Batt. Sol. Cells, 5* (1984) 190.
10 S. Okazaki, S. Higuchi and S. Takahashi, *J. Electrochem. Soc., 132* (1985) 1516.
11 S. Higuchi, S. Okazaki, Y. Takada, O. Nakamura, I. Ogino and S. Takahashi, *Denki Kagaku, 53* (1985) 472.
12 O. Nakamura, S. Okazaki, S. Higuchi and S. Takahashi, *J. Power Sources, 17* (1986) 295.
13 S. Okazaki, S. Takahashi and S. Higuchi, *Prog. Batt. Sol. Cells, 6* (1987) 106.
14 M. Futamata and S. Takahashi, *J. Test. Eval., 16* (1988) 345.
15 M. Futamata, S. Higuchi, O. Nakamura, I. Ogino, Y. Takada, S. Okazaki and S. Takahashi, *J. Power Sources, 24* (1988) 31.
16 O. Nakamura, S. Okazaki, M. Futamata, S. Higuchi and S. Takahashi, *54th Annu. Meet. Electrochem. Soc. Jpn., Osaka, 1987.*
17 S. Higuchi, M. Futamata, Y. Takada, I. Ogino, O. Nakamura and S. Takahashi, *28th Battery Symp. in Japan, Tokyo, 1987.*